

# Synthesis, Characterization, and Degradation of a Novel L-Tyrosine-Derived Polycarbonate for Potential Biomaterial Applications

Huang Xia,<sup>1</sup> Zheng Yuan Suo,<sup>2</sup> Gao Ji Qiang,<sup>1</sup> Cheng Jia Chang<sup>1</sup>

<sup>1</sup>State Key Laboratory for the Mechanical Behavior of Materials, Xi'an Jiaotong University, Xi'an 710049, People's Republic of China

<sup>2</sup>School of Science, Xi'an Jiaotong University, Xi'an 710049, People's Republic of China

Received 14 January 2007; accepted 29 December 2007

DOI 10.1002/app.28755

Published online 11 August 2008 in Wiley InterScience (www.interscience.wiley.com).

**ABSTRACT:** A novel class of pseudo-poly(amino acid)s was synthesized with a cyclic dipeptide as new diphenole. Nonpeptide bonds alternating with a peptide bond structure were introduced into the backbone of the pseudo-poly(amino acid)s. The cyclic dipeptide in this study was obtained from natural L-tyrosine. L-Tyrosine is a major nutrient amino acid with a phenolic hydroxyl group, so a polycarbonate derived from the cyclic dipeptide should possess more optimum mechanical properties, bioactivity, and biocompatibility. The hydrolytic specimen of the resulting polycarbonate was prepared by a modified solvent evaporation process. Under strongly alkaline conditions, degradation testing was performed. The tyrosine-derived polycarbonate possessed a low glass-transition temperature value and a high thermal decomposition temperature value, which formed a broad mean thermal proc-

essing range. The most important results of our study were the effects of the polycarbonate degradation on the local pH values, which were smaller than those of other biodegradable polymers [e.g., poly(lactic acid), poly(glycolic acid), and poly(lactic glycolic acid)]. The synthesized polymer and cyclic dipeptide were characterized with Fourier transform infrared, <sup>13</sup>C-NMR, and <sup>1</sup>H-NMR spectroscopy to determine their chemical structures; by differential scanning calorimetry and thermogravimetric analysis to determine the thermal properties of the polymer; by gel permeation chromatography to determine the polymer's molecular weight; and by X-ray diffraction to determine the polymer's morphology. © 2008 Wiley Periodicals, Inc. *J Appl Polym Sci* 110: 2168–2178, 2008

**Key words:** biodegradable; degradation; polycarbonate

## INTRODUCTION

Since Kohn and Langer<sup>1</sup> presented a new group of potential implant biomaterials, pseudo-poly(amino acid)s, in which the functional groups on the amino acid were used to link individual amino acids or dipeptides via nonamide bonds in 1984, L-tyrosine-based pseudo-poly(amino acid)s have been extensively researched.<sup>2,3</sup> Kohn and Bourke developed a library of diphenolic monomers based on L-tyrosine and corresponding polyiminocarbonates,<sup>4,5</sup> polycarbonates,<sup>1,6–9</sup> and polyarylates.<sup>10,11</sup> All of the L-tyrosine-based polymers possess nonamide linkages alternating with amide linkages in the backbone and, hence, are named pseudo-poly(amino acid)s. The introduction of the nonamide linkages has been found to provide a way for improving the engineering properties of such polymers, such as solubility in common organic solvents, hydrolytic degradability, and thermal mold ability.<sup>12</sup> Gupta

and Lupina<sup>12,13</sup> developed a diphenolic monomeric molecule by using carbodiimide-mediated solid-phase synthesis techniques. The monomeric molecule was polymerized to yield novel biodegradable polyphosphates that contained peptide linkages and phosphoester linkages alternating in the polymer backbone. The results of differential scanning calorimetry (DSC) revealed that the polymers were thermally processable at much lower temperature ranges of 35–45°C. There exist the possible hydrolytic degradability of the phosphoester linkage and the possible enzymatic degradability of the peptide linkage in the polymer backbone.

The peptide in the polymer backbone mentioned previously was all linear. The use of the cyclic peptide as a monomer to synthesize pseudo-poly(amino acid)s has so far not been studied in the field of medical implant materials.

Linear peptides by natural L-amino acids are generally not suitable for use as drugs carriers because of their poor oral availability and enzymatic degradation.<sup>14</sup> Cyclic peptides are playing more and more important roles in biological modeling, pharmaceutical design, nanomolecular devices, biological sensors,

Correspondence to: H. Xia (happyxia@163.com).

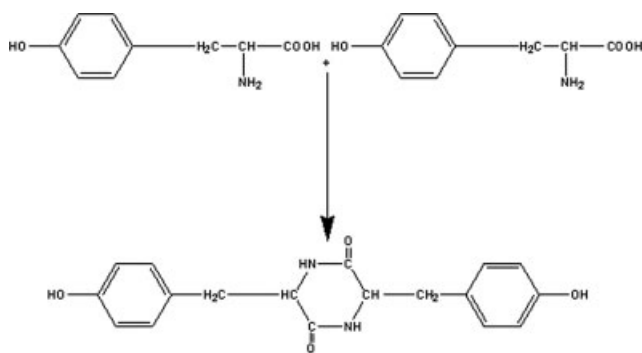


**Figure 1** Representative progress for the formation of the L-tyrosine-based diphenolic molecular cyclic dipeptide.

and catalysts because of their stable structural characteristics and bioactivity.<sup>15</sup> Cyclic dipeptides are of wide interest as potential pharmaceuticals, protein degrade products, and models in peptide chemistry. They have lots of physiological functions and curatorial worthiness and are more steady than linear peptides. Cyclic dipeptides are the simplest members of the prevalent cyclic peptide family found in nature. Many natural cyclic dipeptides have distinct bioactivities that play a vital role in the course of life. Cyclic dipeptides have a high stability because their structures take on the dioxo-piperazine framework. Because of special spatial conformations, cyclic peptides have shown potential in many areas, including chemistry, pharmaceutical chemistry, biochemistry, and the life sciences.<sup>16,17</sup> The cyclic dipeptide this study was derived from L-tyrosine, so the cyclic dipeptide had aromatic and ring conformations. We expected that the polycarbonate derived from this cyclic dipeptide would possess great mechanical properties, stability, and bioactivity.

So far, the Food and Drug Administration approved biodegradable polymers such as poly(glycolic acid), poly(lactic acid), and their copolymers

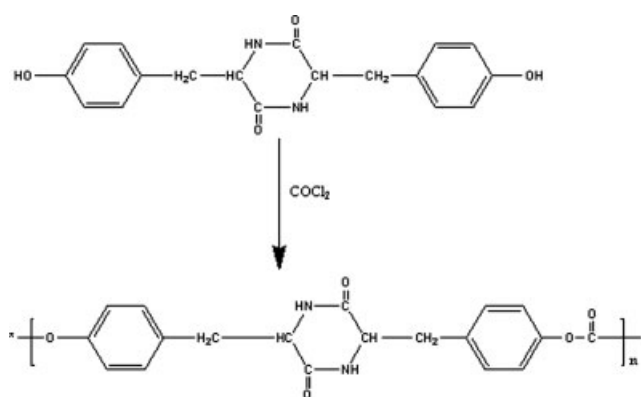


**Figure 2** Synthesis of the L-tyrosine-based polycarbonate from the cyclic dipeptide.

have been found to have adverse tissue reactions. The acidic degradation products of these polymer limit their applications.<sup>13</sup> Therefore, we designed a novel biodegradable polycarbonate whose degradation products are less acidic than those of poly(lactic acid), poly(glycolic acid), and so forth.

The synthesis and applications of a cyclic dipeptide based L-tyrosine are discussed in this article. This cyclic dipeptide was polymerized in the presence of triphosgene. The cyclic dipeptide and polycarbonate were characterized by <sup>13</sup>C-NMR, <sup>1</sup>H-NMR, and Fourier transform infrared (FTIR) spectroscopy to determine their chemical structures. DSC, thermogravimetric analysis (TGA), gel permeation chromatography (GPC), and X-ray diffraction (XRD) were performed to determine the polymer's physico-chemical properties.

## EXPERIMENTAL

### Materials

L-Tyrosine, ethane-1,2-diol, ethanol, triphosgene, methylene chloride, hexane, NaOH, triethylamine, poly(vinyl chloride), and CH<sub>2</sub>Cl<sub>2</sub> were used. All solvents were high-performance liquid chromatography grade.

The monomer and polymer were analyzed by <sup>13</sup>C-NMR, <sup>1</sup>H-NMR, and FTIR spectroscopy to determine their chemical structures. The polymer was also analyzed by GPC for to determine the molecular weight distribution with respect to polystyrene standards. The thermal transition properties of the polymers were studied by DSC to determine their glass-transition temperature's (*T<sub>g</sub>'s*) and by TGA to determine their thermal degradation temperature ranges.

### Measurements

The synthesized monomer and polymer were analyzed by <sup>1</sup>H-NMR and <sup>13</sup>C-NMR spectroscopy on a Bruker AV 300 NMR spectrometer and by FTIR on a

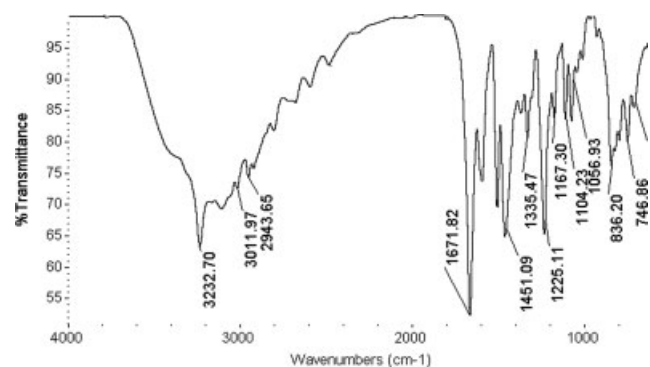


**Figure 3** FTIR spectrum for the synthesized monomer: cyclic dipeptide.

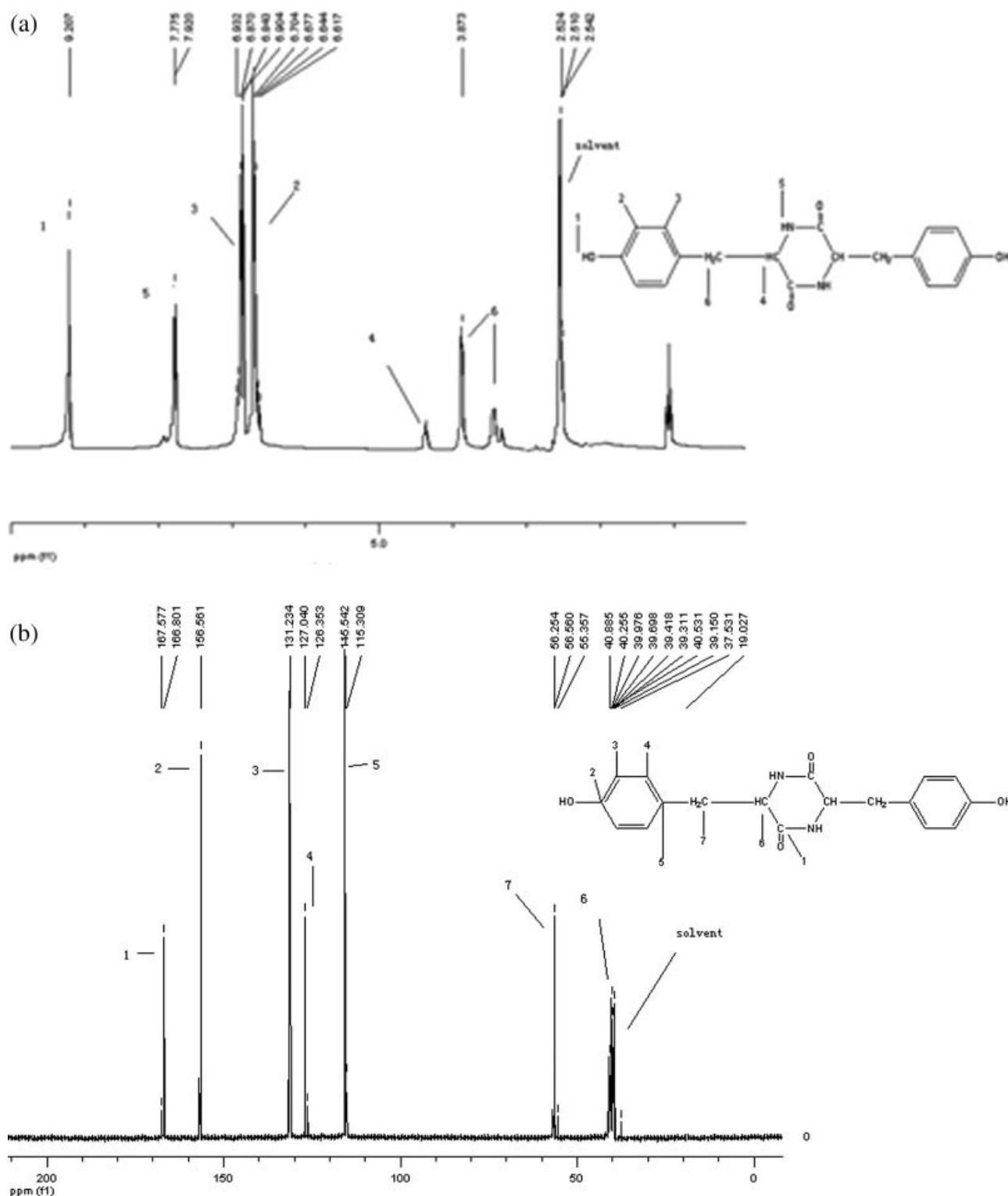


**Figure 4** (a)  $^1\text{H-NMR}$  and (b)  $^{13}\text{C-NMR}$  spectra of the cyclic dipeptide.

Nicolet Nexus (USA) spectrophotometer to determine their chemical structures. The polymer was also analyzed by GPC (with a PLGPC-50 instrument, Waters-Breeze, Waters Co., USA). The eluting solvent was dimethyl sulfoxide (DMSO) with 2.441-g/L LiCl and a flow rate of 0.6 mL/min. The tempera-

ture was  $50^\circ\text{C}$  for the molecular weight distribution with respect to the poly(ethylene glycol) standard. The thermal transition properties of the polymer were studied by DSC (with a TA model 2920 MDSC instrument, USA) to determine  $T_g$  and by TGA (with a TA model 2920 TGA instrument, USA) to

TABLE I  
Representative  $^1\text{H-NMR}$  and  $^{13}\text{C-NMR}$  Characteristic Chemical Shift Assignments of the Cyclic Dipeptide

$^{13}\text{C-NMR}$

Carbon	Chemical shifts (ppm)	Carbon	Chemical shifts (ppm)
1. C(N)=O	167.577, 166.801	5.	127.040, 126.353
2.	156.561	6. CH	40.885
3.	131.234	7. CH <sub>2</sub>	56.560, 56.254, 55.357
4.	115.542, 115.309		

$^1\text{H-NMR}$

Hydrogen	Chemical shifts (ppm)	Hydrogen	Chemical shifts (ppm)
1. Ph-OH	9.207	4. CH	3.873
2.	6.704, 6.677, 6.644, 6.617	5. NH	7.920, 7.775
3.	6.932, 6.904, 6.870, 6.843	6. CH <sub>2</sub>	2.542, 2.524, 2.510

determine the thermal degradation temperature ranges. Also used were magnetic stirring and a frozen, dry, temperature-corrected pH probe.

### Monomer synthesis

The cyclic dipeptide used as the diphenolic monomer was synthesized from L-tyrosine. A mixture of L-tyrosine and dry ethane-1,2-diol was allowed to reflux for 24 h. After cooling, the deposited off-white solid was recrystallized from ethanol.<sup>18</sup> The diphenolic monomer was synthesized according to Figure 1. The cyclic peptide yield was 61%.

### Polymer synthesis

The polycarbonate was synthesized from cyclic dipeptide based L-tyrosine. Because of the insolubility of the cyclic dipeptide in common organic solvents, the interfacial technique described by Pulpura and Kohn<sup>8</sup> was used.<sup>19,20</sup>

### Interfacial polymerization

An amount of 10 mmol of the monomer (3.260 g) was dissolved in 70 mL of 1-mol/L NaOH solution in a three-necked flask equipped with powerful overhead stirring. Methylene chloride (70 mL) was added to

the flask. With vigorous stirring, a solution of 8.41 mmol of triphosgene (2.5 g) in 70 mL of methylene chloride was slowly dropped into the reaction mixture. An amount of 0.50 mg of triethylamine dissolved in 5 mL of methylene chloride was added, and the mixture was stirred for 40 min. The polymer was completely precipitated by the addition of hexane and collected by filtration. The polymer was washed extensively with water until the washings were neutral and then dried to a constant weight under high vacuum. The polymer was synthesized according to Figure 2. The yield of polycarbonate was 67%.

### Hydrolytic degradation studies

#### Preparation of the specimens

The specimens were prepared by a modified solvent evaporation process.<sup>21</sup> Briefly, 0.2 g of polymer was dispersed in 4 mL of  $\text{CH}_2\text{Cl}_2$  with 0.3 g of LiCl with magnetic stirring for 90 s at 7500 rpm. The polymer dispersion was added to 20 mL of an aqueous 1% poly(vinyl alcohol) solution and homogenized for an additional 90 s at 7500 rpm to form an emulsion. The emulsion was added to 300 mL of a 0.1% poly(vinyl alcohol) solution that was continuously stirred for 3 h at room temperature to evaporate the organic solvent.

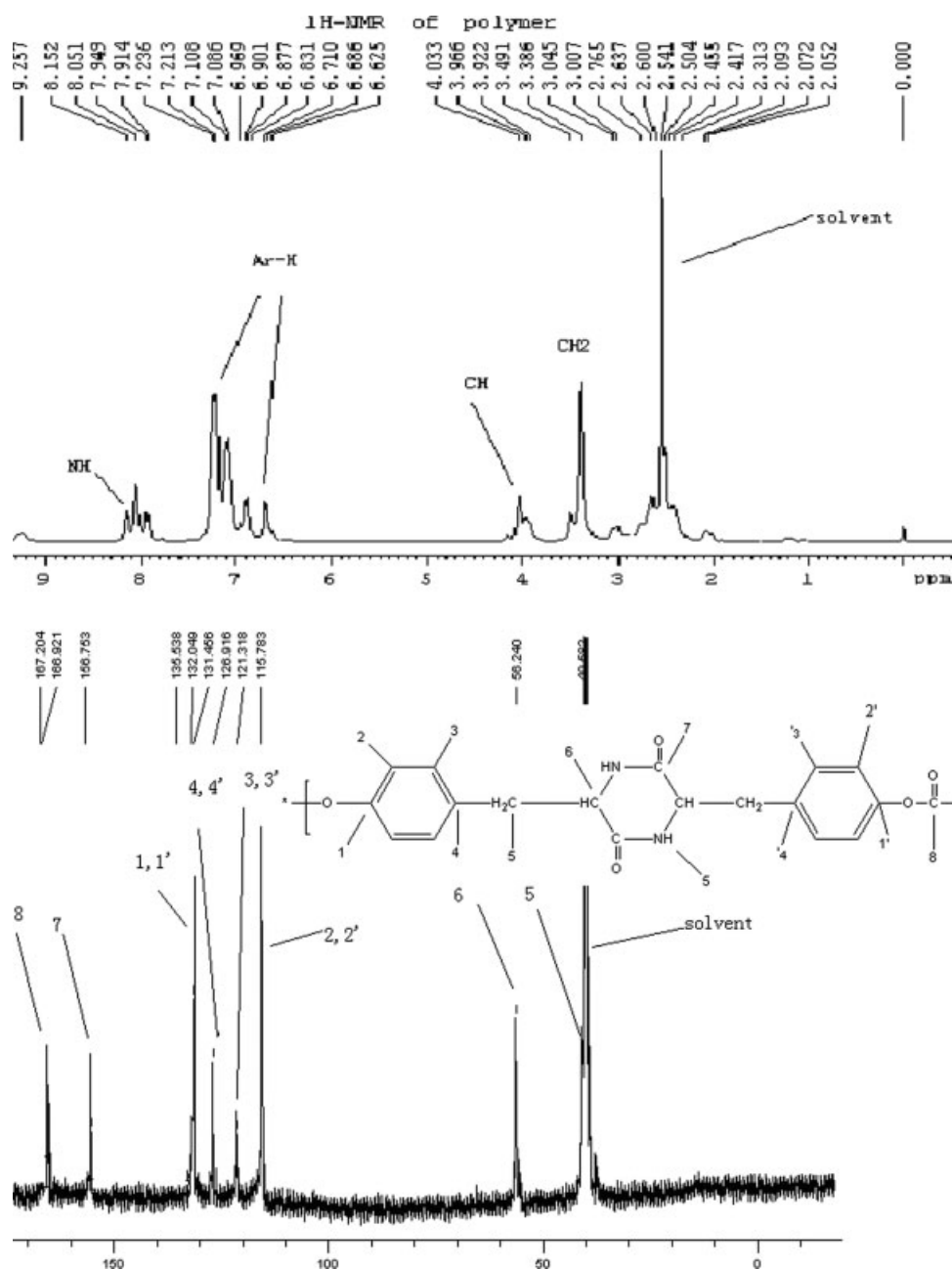


Figure 5 (a) <sup>1</sup>H-NMR and (b) <sup>13</sup>C-NMR spectra of the L-tyrosine-based polycarbonate.

White spongy precipitates were formed, which were isolated by filtration, washed repeatedly with distilled water, and then freeze-dried for 48 h. The specimens were stored at room temperature before use.

#### Hydrolytic degradation of the polycarbonate specimen under alkaline conditions

Information about hydrolytic degradation can be obtained under alkaline conditions. The four specimens were each placed in numbered culture dishes. Each dish was filled with 15–20 mL of a NaOH solu-

tion (1 mol/L) and subjected to a temperature of 37°C. At specific time intervals, the polymer samples were taken out of the dishes, gently placed on filter paper, and immediately weighed to determine the amount of absorbed water in each specimen. The weight of each specimen and the solution pH in each dish was measured and recorded. The morphology change of the polycarbonate specimen was observed by scanning electron microscopy (SEM). The bulk hydrophilicity of the polycarbonate was quantified by the measurement of the amount of water that the specimen absorbed at 37°C.

TABLE II  
Representative  $^1\text{H-NMR}$  and  $^{13}\text{C-NMR}$  Characteristic Chemical Shift Assignments of  
the Tyrosine-Derived Polycarbonate

$^1\text{H-NMR}$			
Hydrogen	Chemical shifts (ppm)	Hydrogen	Chemical shifts (ppm)
1. 1'-Ph-H	7.236–7.213	4. CH	4.033
2. 2'-Ph-H	6.969–6.877	5. NH	8.152
3. $\text{CH}_2$	3.045		

$^{13}\text{C-NMR}$			
Carbon	Chemical shifts (ppm)	Carbon	Chemical shifts (ppm)
1. 1'-Ph-C	135.538	5. $\text{CH}_2$	40.582
2. 2'-Ph-C	115.783	6. CH	56.240
3. 3'-Ph-C	121.318	7. $\text{C(N)=O}$	156.753
4. 4'-Ph-C	132.049	8. $\text{C(O)=O}$	167.204

## RESULTS AND DISCUSSION

### FTIR and NMR spectroscopy of the cyclic dipeptide

Starting from L-tyrosine, we prepared a cyclic dipeptide, as described previously. The chemical structure of the monomer was identified by FTIR,  $^1\text{H-NMR}$ , and  $^{13}\text{C-NMR}$  spectroscopy.

Figure 3 shows the FTIR spectrum of the cyclic dipeptide. The characteristic peaks of secondary amine stretching ( $-\text{NH}-$ ) at  $3385.11\text{ cm}^{-1}$  and amide carbonyl stretching [ $\text{C(N)=O}$ ] at  $1666.57\text{ cm}^{-1}$  were evident in the spectrum. The double primary amine peak for L-tyrosine was found to change into a single broad secondary amine peak in the  $3385.11\text{-cm}^{-1}$  region for the synthesized monomer, which indicated the formation of amide ( $-\text{NH}-$ ). Other characteristic bands included  $3201.17\text{ [v(OH)]}$ ,  $3054.01\text{ [v(aromatic CH)]}$ ,  $2943.65$  and  $2864.82\text{ [v(alkyl C-H)]}$ ,  $1508.91$  and  $1442.58\text{ [v(aromatic C-C)]}$ ,  $1377.52$  and  $1330.22\text{ [\delta(OH)]}$ ,  $1240.88\text{ [v(C-O)]}$ ,  $1077.96$  and  $1031.66\text{ cm}^{-1}\text{ [\delta(aromatic CH)]}$ , and  $878.25$  and  $825.69\text{ cm}^{-1}\text{ [\delta(1,4-dibasic benzene)]}$ .

The NMR spectrum of the cyclic dipeptide is shown as Figure 4. The characteristic chemical shift assignments are listed in Table I. The  $^{13}\text{C-NMR}$  spectrum revealed the presence of amide carbonyl carbon peaks in the  $150\text{--}170\text{-ppm}$  region, the presence of connecting phenolic hydroxyl carbon peaks in the  $130\text{--}160\text{-ppm}$  region, the presence of typical aromatic carbon peaks in the  $110\text{--}160\text{-ppm}$  region, and the presence of  $-\text{CH}_2-$  and  $-\text{CH}-$  groups in the

$20\text{--}70\text{-ppm}$  region. The  $^1\text{H-NMR}$  spectrum revealed the presence of phenolic hydroxyl peaks in the  $9.207\text{-ppm}$  region, the presence of a  $-\text{CH}-$  connecting NH chemical shift at  $4.5\text{ ppm}$ , and the presence of a NH chemical shift at  $7.775\text{ ppm}$ . Hence, according to the information provided by FTIR,  $^1\text{H-NMR}$ , and  $^{13}\text{C-NMR}$ , the spectrum supported the expected structure of the cyclic dipeptide, as shown in Figure 4.

### NMR and FTIR spectroscopy of the tyrosine-based polycarbonate

Figure 5 shows the NMR analysis results for the tyrosine-based polycarbonate. The characteristic chemical shift assignments are listed in Table II. The  $^{13}\text{C-NMR}$  spectrum revealed the presence of ester and amide carbonyl carbon peaks in the  $150\text{--}170\text{-ppm}$  region, the presence of typical aromatic carbon peaks in the  $110\text{--}160\text{-ppm}$  region, the presence of

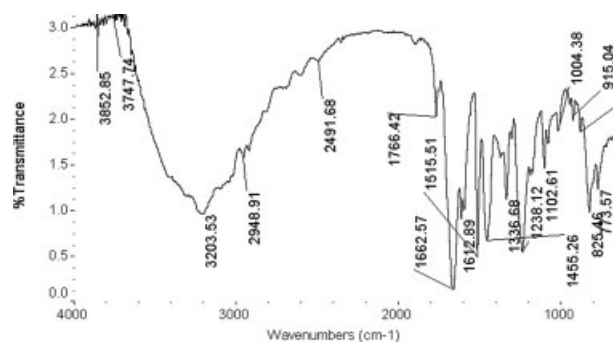
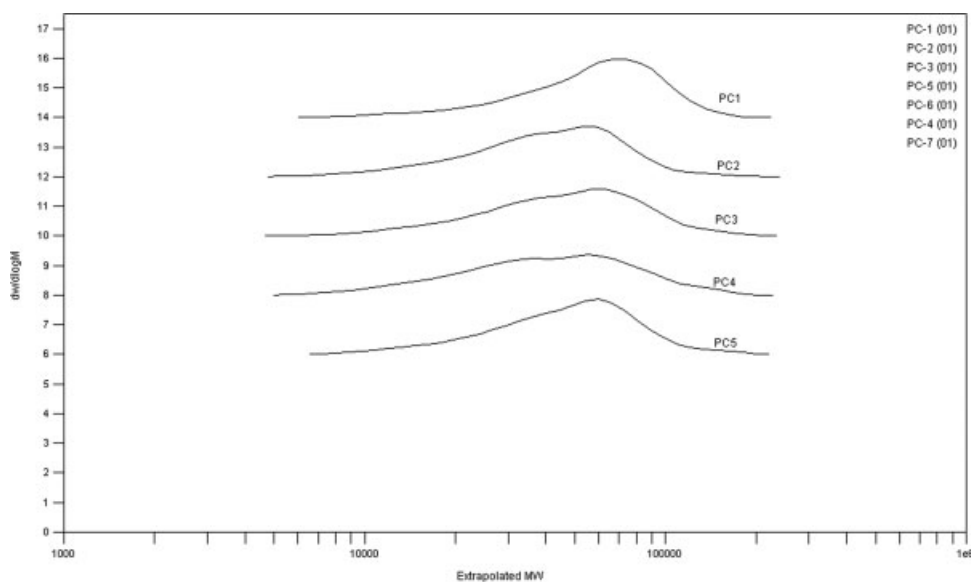


Figure 6 FTIR spectrum of the synthesized L-tyrosine-based polycarbonate.



**Figure 7** Molecular weight distribution of a polycarbonate sample during degradation.

$-\text{CH}_2-$  and  $-\text{CH}-$  groups in the 20–70-ppm region, and the presence of  $\text{C}(\text{O})=\text{O}$  at 156.753 ppm.  $^1\text{H}$ -NMR spectroscopy showed that the chemical shift of  $-\text{OH}$  at 9.207 became slighter than that of the cyclic dipeptide, which indicated the formation of  $\text{C}(\text{O})=\text{O}$ . The peaks at 8.152–7.914 ppm belonged to  $-\text{NH}-$ , those at 7.636–6.625 ppm belonged to the hydrogen from the benzene ring, that at 4.033 ppm belonged to  $-\text{CH}-$ , and that at 3.386 ppm belonged to  $-\text{CH}_2-$ . Hence, the spectrum supported the expected structure of the tyrosine-based polycarbonate repeating unit, as shown in Figure 5.

Figure 6 shows the FTIR analysis results for the polymer. The polymer had characteristic IR absorptions at 3360–3310 (N–H), 2960–2860 (C–H from the cyclic dipeptide), 1773.3 [ $-\text{C}(\text{O})=\text{O}$  carbonate], and

1673  $\text{cm}^{-1}$  [ $\text{C}=\text{O}(\text{N})$ ]. Other characteristic bands included aromatic C–H stretching at about 3045  $\text{cm}^{-1}$ ,  $\text{CH}_2$  scissoring deformation at about 1460  $\text{cm}^{-1}$ , C–C stretching at around 1200–1100  $\text{cm}^{-1}$ , and C–N stretching at 1369.48  $\text{cm}^{-1}$ .

The NMR analysis results and the FTIR analysis results in conjunction confirmed the formation of the tyrosine-based polycarbonate, where the repeating units of the polymer contained an amide (peptide) linkage from the cyclic dipeptide and a carbonate ester linkage from the triphosgene.

#### Molecular weight distribution and thermal properties of the polymer

The molecular weight distribution of the synthesized polymer was determined by GPC techniques with

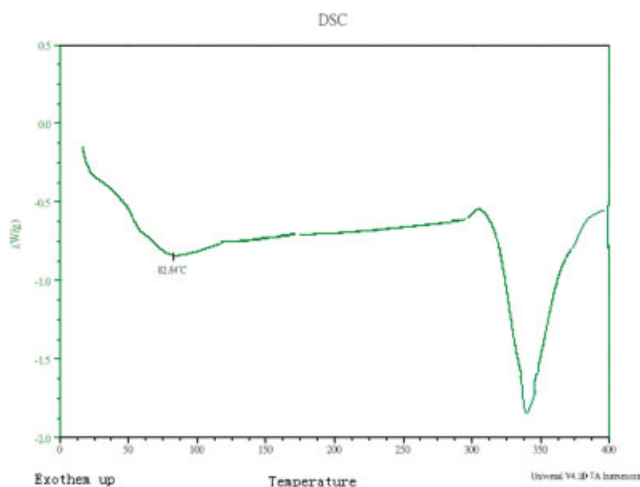


**Figure 8** DSC curve of the L-tyrosine-derived polycarbonate. [Color figure can be viewed in the online issue, which is available at [www.interscience.wiley.com](http://www.interscience.wiley.com).]

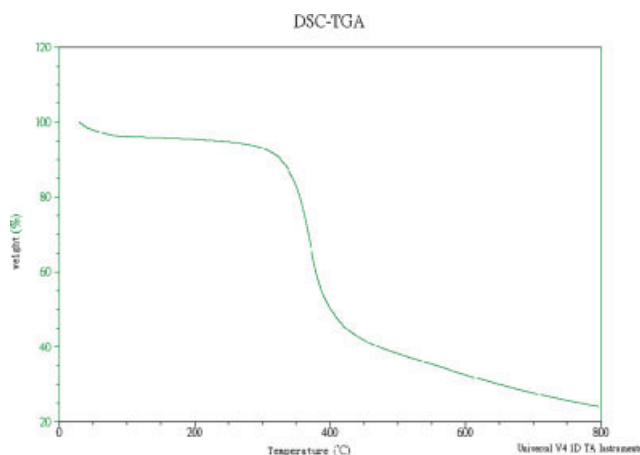


**Figure 9** TGA of the polymer. [Color figure can be viewed in the online issue, which is available at [www.interscience.wiley.com](http://www.interscience.wiley.com).]

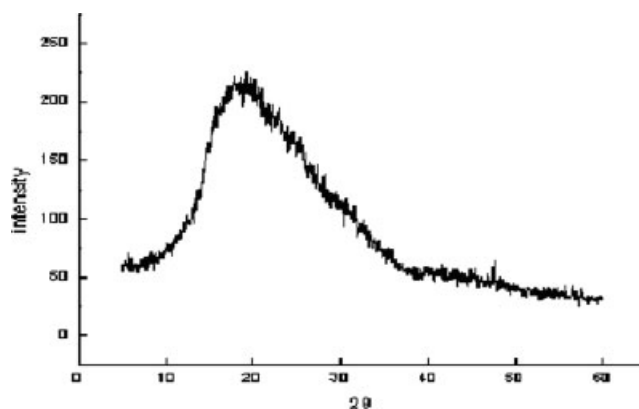


Figure 10 XRD of the polymer.

DMSO as the eluting medium. Figure 7 shows the GPC analysis result for the polymer. From the GPC results, we found that the polymer, with a weight-average molecular weight ( $M_w$ ) of approximately 63,086 Da and a number-average molecular weight ( $M_n$ ) of approximately 36,386 Da, was successfully synthesized. The polydispersity index ( $P_d$ ) of the polymer was 1.7337.

The DSC technique was used to determine the  $T_g$  of the polymer. The heating rate was kept at 10°C/min. Figure 8 shows the DSC analysis results. The thermal degradation temperature range of the polymer was determined by TGA. The heating rate was kept at 10°C/min under a flow of nitrogen. Figure 9 shows the TGA results. The polymer showed  $T_g$  values in the range of 120–122°C. The pure poly(L-tyrosine) showed a slight slope change around 185°C,<sup>12</sup> which implied that it hardly underwent glass transition. For the polymer, the thermal degradation temperature was observed above 350°C. Compared to the pure poly(amino acid)s, the polymer showed the potential for avoiding the risk of thermal degradation. The lower  $T_g$  values and high thermal degradation

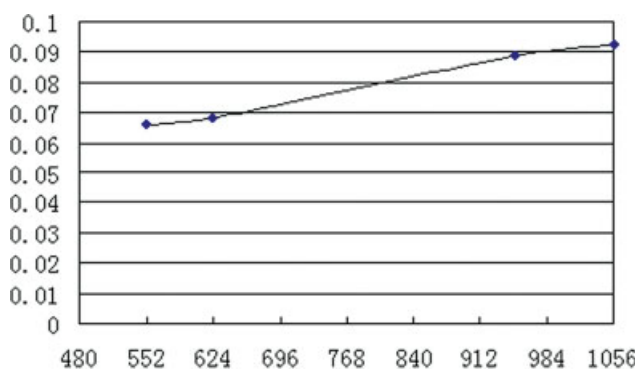


Figure 11 Mass trend curve of the polycarbonate. [Color figure can be viewed in the online issue, which is available at [www.interscience.wiley.com](http://www.interscience.wiley.com).]

TABLE III  
Changes in the Molecular Weight During the Hydrolytic Period

	$M_w$	$P_d$	$M_n$
PC1	63,086	1.7337	36,386
PC2	52,653	1.4677	35,874
PC3	45,041	1.3983	32,211
PC4	46,214	1.4242	32,450
PC5	48,585	1.5564	31,217

tion temperature values suggested a broad thermal processing temperature range. Hence, the L-tyrosine-based polycarbonate could be considered a biomaterial with significant engineering advantages.

The X-ray powder diffraction patterns of the polymer were detected, as illustrated in Figure 10. The XRD curve suggested that the polymer was amorphous. This was in accordance with the low  $T_g$  of the polymer.

Tyrosine-derived polycarbonates possess three potentially hydrolytic bonds: amide, carbonate, and ester bonds.<sup>7</sup> Such carbonate ester linkages were present in the polymer repeating unit, which made the polymer hydrolytically degrading. The peptide linkage in the polymer repeating unit was enzymatically degradable. Hence, the combination with hydrolytic degradability makes this tyrosine-based polycarbonate a potentially biodegradable polymer. The hydrolytic degradation studies of the L-tyrosine-based polycarbonate showed results in accordance with this inference.

#### *In vitro* degradation study of the polycarbonate

##### Weight loss of the specimen

Accelerated hydrolytic degradation was done with a 1-mol/L sodium hydroxide solution for 1056 h. The polycarbonate had hydrolytic bonds in its main backbone. Under alkaline conditions, the degradation of the specimen was represented by weight loss. The weight losses at specific times were recorded. Figure 11 shows the trend curve of the weight loss. As evident from the experiment results, the specimen did not have any obvious weight change over the initial period. In 624 h, the slope of the curve increased, which indicated an increasing rate of degradation. The progress of the degradation became

TABLE IV  
Changes in the pH Value During the Incubation Period

pH	13.69	13.33	13.1	12.86	12.53
Time (h)	0	552	624	950	1056



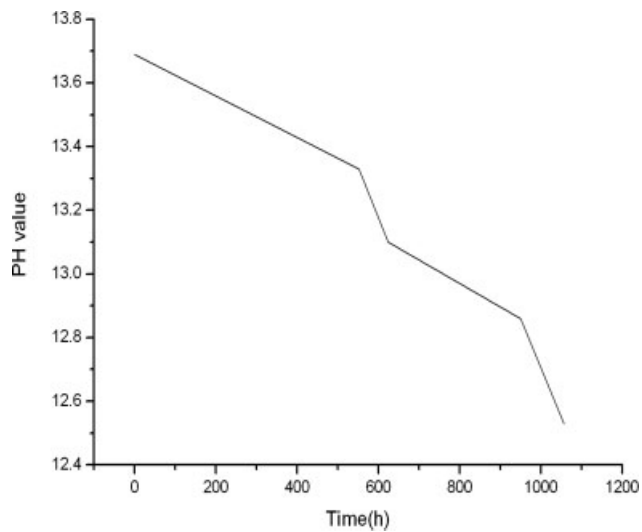


**Figure 12** pH change curve for the degradation solution.

gentle after 984 h. The weight loss was homogeneous during the degradation. The results indicate that the polycarbonate was a surface-eroding biodegradable polymer.

#### Effect of degradation on the molecular weight distribution

The degradation of the polycarbonate was monitored with GPC to determine the changes in molecular weight that the samples underwent during the incubation period.  $M_n$  of polycarbonate was about 60,000, and the polydispersity was about 1.7337, which was typical for condensation polymerization (Table III). Figure 7 shows the evolution of the  $M_w$  distribution during the hydrolysis of the polycarbonate. Table III shows the decay in the  $M_n$ ,  $M_w$ , and  $P_d$  data. No significant changes in the molecular weight of the samples were observed. We observed a decrease in the molecular weight distribution at first, which then increased. The value of  $P_d$  decreased because that part of low-molecular-weight degraded at first. The value of  $P_d$  increased because that the oligomers produced by hydrolysis were insoluble in water. In this hydrolytic degradation experiment, the weight loss of the all samples was more obvious than the change in molecular weight. So the degradation model of the polycarbonate was surface erosion.

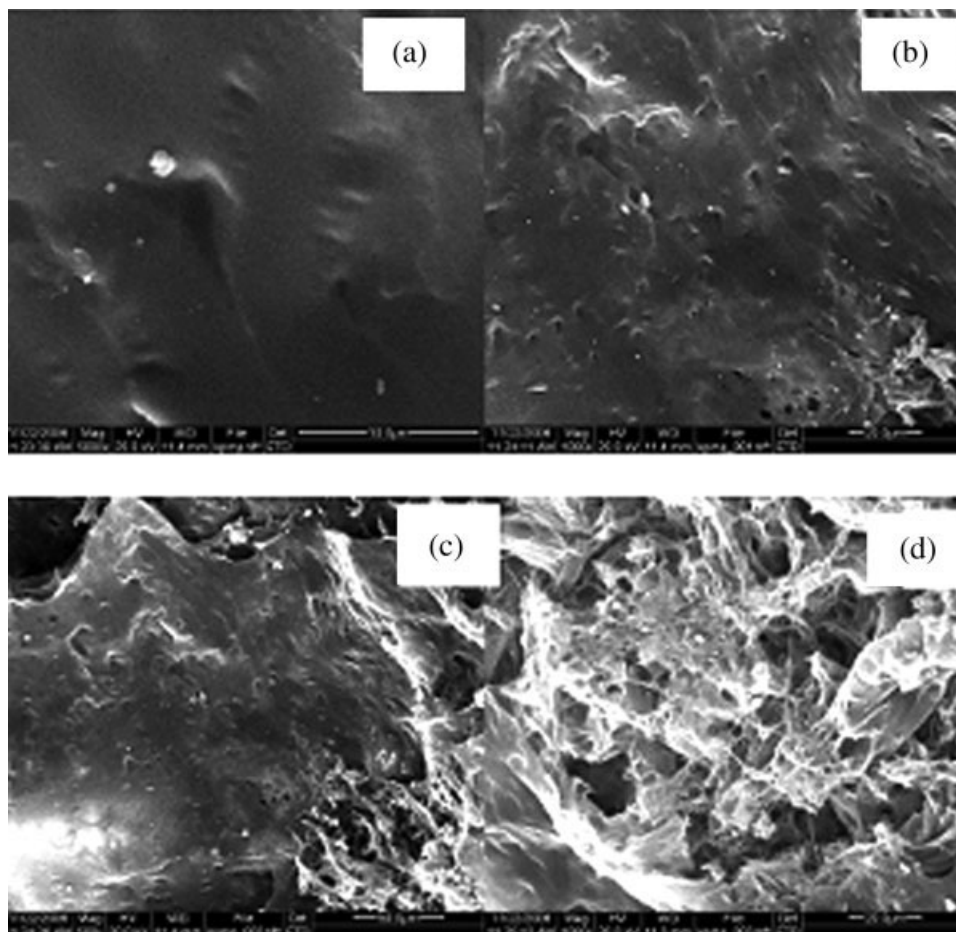


**Figure 13** SEM images of the polycarbonate: (a) the initial specimen and the specimen after degradation times of (b) 552, (c) 950, and (d) the specimen after degradation for 1056 h.

### Effect of degradation on the local pH

Lots of biodegradable polymers, such as poly(lactic acid), poly(glycolic acid), and poly(lactic glycolic acid), produce degradation products that can change the local pH of the environment in which they are degrading.<sup>13,22</sup> In fact, these changes have adverse nonspecific inflammatory effects in the physiological environment, especially in osseous tissue.

To examine the degradation properties of the polymer, a thermostat was brought to the desired temperature (37°C), and each dish contained the sodium hydroxide solution (1 mol/L). At specific intervals of time (0, 552, 624, 950, and 1056 h), the solution was measured with a temperature-corrected pH probe.

Figure 12 shows the local pH change due to the degradation of the polymer. As evident from the figure, the local pH decreased slightly during the degradation. This signified that the polymer released acidic degradation products, but they did not obviously affect the local pH. The pH change value of the polymer was found to be 1.16 over 1056 h. It was reported elsewhere<sup>13</sup> for poly(lactic glycolic acid) that pH change value was 3.5 over 150 h. It can be expected that in osseous tissue engineering related applications, this polycarbonate would have a lower probability of eliciting inflammatory reactions.

### Morphological changes and water uptake of the specimens

It was necessary to study the morphological changes of the polycarbonate specimen. Figure 13 shows the SEM images of the specimen after different periods of degradation. As shown in this figure, no obvious changes were evident on the surface during the initial 552 h. The surface became porous after 950 h of degradation. A useful feature of the degradation process was that the specimens retained their physical integrity. Compared to other biodegradable polymers, the tyrosine-derived polycarbonate was more stable. This depended on the diphenol structure in the polymer backbone. The natural amino acid L-tyrosine is a major nutrient with a phenolic hydroxyl group.<sup>6</sup>

The water uptake of the specimen was investigated in deionized water at 37°C. The specimen was incubated for 8 weeks. The initial weight ( $m_0$ ) and absorption weight ( $m_1$ ) of the specimen were recorded. The water uptake of the polycarbonate was calculated as follows:

$$\text{Water uptake(\%)} = (m_1 - m_0)/m_0$$

Over a period of 8 weeks, the polycarbonate absorbed 5% water.

## CONCLUSIONS

A novel biodegradable polycarbonate was synthesized via the interfacial polymerization of a cyclic dipeptide and BTC. The cyclic dipeptide was synthesized from the natural amino acid L-tyrosine, so the chemical structure of the L-tyrosine-derived polycarbonate was determined by detailed analyses with <sup>13</sup>C-NMR, <sup>1</sup>H-NMR, and FTIR techniques. DSC analyses revealed that the polymer was potentially thermally processable at lower temperatures, compared to the high temperature necessary for pure poly(L-tyrosine). Because of the possible hydrolytic degradability of the carbonate-ester linkage and the possible enzymatic degradability of the peptide linkage in the polymer backbone, accelerated hydrolytic degradation was done to examine the properties of degradation. The degradation product of the polymer was found to have a negligible effect on local pH. Because of the slow degradation and surface erosion of the polycarbonate, it may be used in degradable bone screws or bone pins. Hence, in the light of these results, the polycarbonate fulfills all the requirements for biodegradable polymers.

The most significant advantages of the polycarbonate are as follows:

1. It is derived from a cyclic dipeptide and possesses great bioactivity, biocompatibility, enzymatic degradation, and so on.
2. There are aromatic units and six-membered heterocycles in its main chain, so it possesses great mechanical properties.
3. The degradation model of the polycarbonate is surface erosion. The mechanical property changes in the sample were slight during degradation.
4. The lower  $T_g$  values and high thermal degradation temperature values suggest a broad thermal processing temperature range.

So this tyrosine-based polycarbonate is a promising biomaterial and deserves further investigation into its possible biomaterial applications.

## References

1. Kohn, J.; Langer, R. *Polymeric Materials, Science and Engineering*; American Chemical Society: Washington, DC, 1984; Vol. 51, p 119.
2. Kohn, J.; Langer, R. *J Am Chem Soc* 1987, 109, 817.
3. Ertel, S. I.; Kohn, J. *J Biomed Mater Res* 1994, 28, 919.
4. Pulapura, S.; Li, C.; Kohn, J. *Biomaterials* 1990, 11, 666.
5. Kohn, J. *Trends Polym Sci* 1993, 1, 206.
6. Bourke, S. L.; Kohn, J. *Adv Drug Delivery Rev* 2003, 55, 447.
7. Tangpasuthadol, V.; Pendharkar, S. M.; Kohn, J. *Biomaterials* 2000, 21, 2371.
8. Pulapura, S.; Kohn, J. *Biopolymers* 1992, 32, 411.

9. Tangpasuthadol, V.; Shefer, A.; Hooper, K. A.; Kohn, J. *Bio-materials* 1996, 17, 463.
10. Puma, M.; Suarez, N.; Kohn, J. *J Polym Sci Part B: Polym Phys* 1999, 37, 3504.
11. Suarez, N.; Brocchini, S.; Kohn, J. *Polymer* 2001, 42, 8671.
12. Gupta, A. S.; Lopina, S. T. *Polymer* 2004, 45, 4653.
13. Gupta, A. S.; Lopina, S. T. *Polymer* 2005, 46, 2133.
14. Cabrele, C.; Langer, M.; Beck-Sickinger, A. G. *J Org Chem* 1999, 64, 4353.
15. Kimura, Y.; Tani, K.; Kojima, A.; et al. *Phytochemistry* 1996, 41, 665.
16. (a) Wipf, P. *Chem Rev* 1995, 95, 2115; (b) Chandan, P. *Peptides* 1995, 16, 151.
17. Li, T.; Han, B.; Zhu, H.; Song, G.; Wang, J. *Chem Ind Times* 2004, 18, 37.
18. Cook, B.; Hill, R. R.; Jeffs, G. E. *J Chem Soc Perkin Trans* 1992, 10, 1199.
19. Merrill, S. H. *J Polym Sci* 1961, 55, 343.
20. Goldberg, E. P. *J Polym Sci Part C: Polym Symp* 1964, 4, 707.
21. O'Donnell, P. B.; McGinity, J. W. 1997, 28, 25.
22. Mao, H.; Leong, K. W. U.S. Pat. 5,912,225 (1999).